J|A|C|S
ARTICLES
Published on Web 11/02/2002

Stereocartography: A Computational Mapping Technique That Can Locate Regions of Maximum Stereoinduction around Chiral Catalysts

Kenny B. Lipkowitz,* Cedric A. D'Hue, Taka Sakamoto, and Jonathan N. Stack

Contribution from the Department of Chemistry, Indiana University-Purdue University at Indianapolis (IUPUI), 402 N. Blackford Street, Indianapolis, Indiana 46202

Received May 22, 2002. Revised Manuscript Received July 18, 2002

Abstract: A hypothesis concerning asymmetric induction by chiral catalysts is posited, tested, and found to be valid. The hypothesis states that chiral catalysts that are efficient at inducing asymmetry will have their region of maximum stereoinduction spatially congruent with the site of chemistry but inefficient catalysts will not. A simple mapping strategy (stereocartography) is used to assess where the region of maximum stereoinduction is located around a given catalyst. The protocol compares interaction energies between mirror image probes at each point in space around the catalyst being considered. The probes are models of the actual transition states of the reaction being catalyzed by a particular catalyst. The hypothesis was tested on three Diels−Alder reactions. Seventeen of the eighteen catalysts conform to the hypothesis. The idea of using this as a catalyst design tool is presented.

Introduction

Chirality transcends traditional boundaries separating subdisciplines of the chemical sciences. The large number of scientific studies focusing on the topic of chirality has now thrust it into the scientific forefront, especially in biological and organic chemistry but more recently in inorganic and organometallic chemistry. Reflecting interest in chirality are new journals dedicated to this topic including: *Tetrahedron: Asymmetry*, *Enantiomer*, and *Chirality*, all of which complement existing journals that are themselves replete with papers on chirality. Workshops, symposia, and conferences dedicated to chirality are now common and popular. Further attesting to the significance of this topic was a series of feature articles in *Chemical and Engineering News* laying bare the fact that a whole new industry based on chirality now exists.[1] This industry, designated as "chiroscience", is a young but robust industry linking science and technology with chemistry and biology. A visual illustration of the growth in research dedicated to topics in chirality is shown in Figure 1. The number of hits from a search of the chemical abstracts is plotted yearly from 1975. The first plot (**1** on the horizontal axis) is for the key word "chiral". The growth in these publications far exceeds the annual increment of CAS citations. Also plotted (**2** and **3**, respectively) are the number of citations in the area of "asymmetric synthesis" and "chiral catalysis", the focus of this paper.

The emphasis of chemical research on catalysts capable of asymmetric induction is understandable, especially from an industrial perspective where one wants high yields of highly stereoselective reactions using inexpensive reagents and where the catalysts maintain their integrity for indefinite time periods. Many advances were made in this regard and those developments were highlighted in numerous reviews (since 1995 there have been in excess of 100 reviews written annually on the topic) culminating in the state-of-the-art compendium *Comprehensive Asymmetric Catalysis* published in 1999.[2] These summarizing publications indicate that we are far from achieving

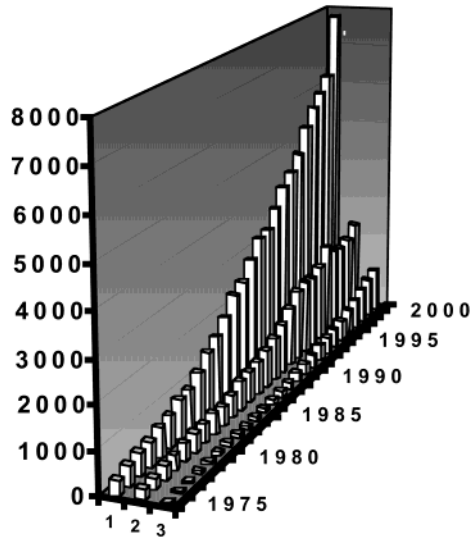

Figure 1. Number of hits from a SciFinder search versus year for keywords: "chiral", **1**, "asymmetric synthesis", **2**, and "chiral catalysis", **3**.

Address correspondence to this author. E-mail: lipkowitz@chem.iupui.edu.

(1) (a) Stinson, S. C. *Chem. Eng. News* **2001**, 79−97. (b) Stinson, S. C. *Chem. Eng. News* **1995**, 44−74. (c) Stinson, S. C. *Chem. Eng. News* **1994**, 38−72. (d) Stinson, S. C. *Chem. Eng. News* **1993**, 38−65.

(2) *Comprehensive Asymmetric Catalysis*; Jacobsen, E. N., Pfaltz, A., Yamamoto, H., Eds.; Springer-Verlag: New York, 1999; 3-vols.; ISBN 3-540-64336-2.

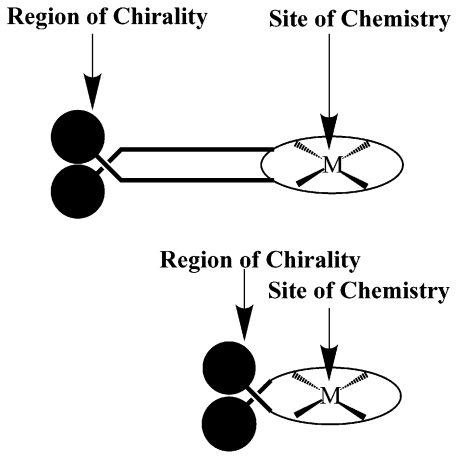

Figure 2. Schematic representation of the concept discussed in this paper. Top: A situation where the site of chemistry is far removed from the stereoinducing portion of a chiral ligand. Because the intermolecular forces fall off quickly, the stereodiscriminating forces needed for asymmetric induction are weak and little enantiomeric excess is anticipated. Bottom: A situation where the site of chemical reaction is near the stereoinducing portion of a chiral ligand. Here, the enantiodiscriminating forces are maximized thus allowing the catalyst to be effective.

the industrial goals desired for chiral catalysts; while some catalysts perform well, most do not, even after extensive "tweaking". Moreover, what is learned from optimization of catalytic performance in one system usually does not transfer well to other systems; there is a clear lack of guidelines or rules for chiral catalyst design.

In this paper, we set out to prove or disprove the following hypothesis: *Maximum asymmetric induction by a catalyst is achieved when the region of greatest stereoinduction is spatially congruent with the site of chemistry*. What we are saying here is that the location in which bond making and bond breaking takes place on a catalyst ought to be more than just chiral: That location should be the most stereoinducing region to ensure the catalyst is as efficient as possible at transferring chirality. A cartoon representing this intuitive concept is presented in Figure 2.

In this diagram, we depict a typical catalyst having a metal coordinated to a ligand that is either asymmetric or dissymmetric. The site of chemistry is thus somewhere near the metal center. The intermolecular interactions between a chiral ligand and the reagents undergoing a chemical transformation at the metal center fall off as $1/r$ (ion−ion) to $1/r^2$ (ion−dipole) to $1/r^3$ (dipole−dipole) to $1/r^6$ (dispersion). Thus, it is clear that when the stereoinducing portion of the ligand is too distant from the metal site, little or no asymmetric induction is possible because both enantiomeric transition states will have the same or similar energies. This situation is represented in the top of Figure 2. Contrarily, having the "chirality" at the reaction site ensures an asymmetric environment for the reactants that will desymmetrize an otherwise degenerate set of reaction coordinates thus providing one enantiomeric product in excess of the other. The efficiency of this process is commonly presented as the enantiomeric excess, ee.

In the research described below, we evaluate the propinquity of these two regions (computationally) for a set of well-characterized chiral catalysts. Our ultimate goal from this research is to quantify a loosely defined, intuitive concept that is otherwise prone to subjective interpretation by research

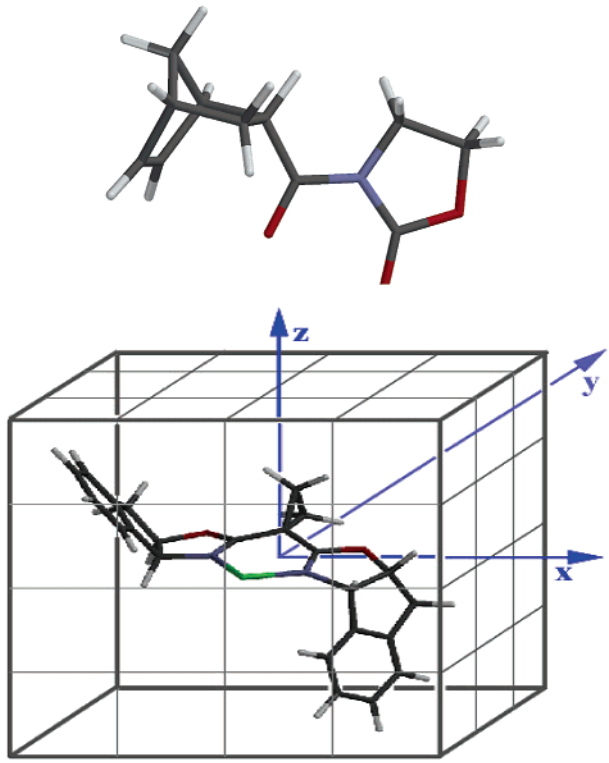

Figure 3. Top: Example of one of the transition-state probes used in this research project. Bottom: A chiral ligand ensconced in a uniform three-dimensional grid of points. The grid mesh used in this paper is much finer than that depicted here. At each grid point, a Boltzmann weighted energy is determined between the probe and the catalyst for a large number of probe orientations. Both (R) and (S) antipodes are considered in the calculations.

scientists. We want to quantify such concepts so that ligands for use as asymmetric catalysts could be improved upon, or better yet, be designed de novo; as such, this work would represent a step in the direction of providing general rules or guiding principles for catalyst design.

Methodology

General Procedures. The methodology we develop here involves the mapping of stereodiscriminating regions around a chiral catalyst—hence the term stereocartography. The calculations are done in the following manner. (1) Place the catalyst's center of mass at the origin of a Cartesian coordinate system and place a uniform three-dimensional grid around that catalyst as shown in Figure 3.

(2) Select a chiral "probe" molecule; in our case the probe will be the transition state of the molecules reacting in the presence of the catalyst. (3) Place the "probe" molecule's center of mass at each grid point and compute an intermolecular energy using a suitable force field with electrostatically fitted point charges. At each grid point, a large number of orientations of the probe molecule relative to the catalyst are sampled deterministically and a Boltzmann averaged intermolecular energy is computed for that particular grid point. (4) Repeat these calculations at all grid points (excluding those where interpenetration of molecules would otherwise occur) for the (R) probe and its antipodal (S) form. (5) Generate isodensity contour plots encapsulating grid points of largest difference in energy. Grid points with little or zero energy difference are deemed to be non-stereodifferentiating. Contrarily, those grid points with large energy differences between mirror image probes are considered to be enantiodiscriminating. The centroid of the region displaying the largest difference in transition-state interaction energies is compared to the center of reaction to assess the spatial congruence of those regions.

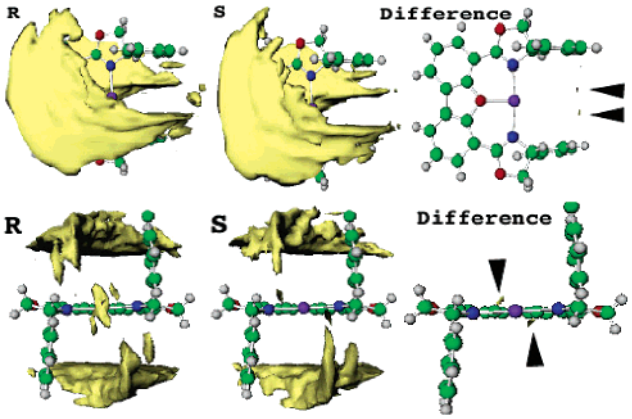

Figure 4. Top view (top panel) and front view looking down the Ni−O bond (bottom panel) of the preferred binding domain of the (R) transition-state probe around the catalyst, the (S) transition-state probe around the catalyst, and the difference map defining the region of greatest stereoinduction.

An example of such a calculation is illustrated in Figure 4. The catalyst depicted is the C_2-symmetric Ni-coordinated, *trans*-chelating, tridentate (R,R)-4,6-dibenzofurandiyl-2,2′-bis(4-phenyloxazoline) of Kanemasa and Curran that catalyzes the cycloaddition of cyclopentadiene with 3-acryloyl-2-oxazolidinone in high yields (96%) and high ee (>99%).[3] The (R) and (S) "probes" for this study are the quantum mechanically derived transition structures corresponding to the preferred *endo* product. The grid spacing for each probe was 0.25 Å and Boltzmann-weighted energies determined from 1728 unique, uniformly sampled orientations were derived for each grid point using the AMBER* potential incorporating quantum mechanically derived, electrostatic potential (ESP) charges.

Shown in Figure 4 are the lowest energy binding regions for the "R" probe, the "S" probe, and the difference plot in which the most stereodiscriminating regions are highlighted. The catalyst structure used for these calculations is a near-C_2-symmetric crystal structure giving a near-2-fold symmetric binding domain. In this particular example, we find the most enantiodiscriminating region in "front" of the catalyst, near the metal center. This result is consonant with our working hypothesis that catalysts with high ee have such stereoinduction regions near the site of chemistry while poor catalysts do not; this and other systems will be described below in detail.

The catalysts used for the calculations described in this paper are derived from the Cambridge Structural Database (CSD)[4] and used directly, or they have been modified and geometry optimized quantum mechanically with a semiempirical Hamiltonian. For each catalyst described below, we indicate how the structure was obtained. The enantiomeric "probes" we are implementing in this mapping procedure correspond to the actual enantiomeric transition states of the reactions being studied rather than some judiciously selected, generic probe molecule that is chiral. We do this because each catalyst will behave differently with each unique set of reactants and we want to capture that specificity for each different and unique chemical reaction being evaluated. This generalizes the procedure and makes it applicable to any catalyst and to any set of reactions. To generate each probe molecule, we compute the transition state for each reaction quantum mechanically, ensuring a single negative eigenfrequency exists. From that is generated the mirror image probe by reflecting atomic coordinates through the XY plane. These probes are then used to compute the intermolecular interactions between catalyst and transition states.

Both catalyst and probes are being treated as rigid body molecules. In some instances, there exist more than a single conformation accessible to the catalyst that must be considered. For such systems, we first carry out a conformational analysis of catalyst to generate a Boltzmann weighted list of conformations. For each conformer of catalyst (and probe), we then carry out the aforementioned rigid-body sampling. Each grid point is thus energy weighted by the likelihood of the catalyst existing in that particular conformational state. For example, if a catalyst has two conformers arising from an ethyl group rotation that are weighted, say, 60% and 40% respectively, the weighting of intermolecular energies at each grid point for each conformer is similarly weighted 60% and 40%. This corresponds to the probes interacting with each conformation of the catalyst in a weighted manner and this way we can account for conformations of both catalyst and probe molecules. Hence, the grid points depicted in this paper are weighted averages accounting for conformational states *and* the large number of orientations of probe molecule with respect to those conformations.

The working philosophy we adopted in this initial study is to compute the transition-state probes for the various reactions under study in isolation. In other words, we do not consider the chiral ligand's influence on the transition state. We do this for two reasons. First, locating transition states for these systems is extremely difficult, especially for reactants that bind monovalently to the metal and which have a wide range of binding orientations to consider. This is a time-consuming exercise with no guarantee that one will be able to locate a transition structure nor with a guarantee that the transition structure found is the correct one. We want to generate a straightforward computational method that one can use to assess whether a proposed catalyst will be efficient or inefficient without needing to compute actual transition structures. Second, we want to use true enantiomeric (mirror image) transition-state probes in our mapping. The actual transition states, bound to a chiral catalyst, are diastereomeric in nature; the two transition states will thus differ in structure somewhat. This raises an issue of how sensitive the results are to differences in geometry of catalyst or transition state. Several tests were done to address this issue and we found that the results do depend on structural changes as expected, but they are not very sensitive to this. For example, using catalysts **2** and **10** described below, the phenyl groups were twisted from their equilibrium geometry stepwise in 2° increments (both in a conrotatory and a disrotatory fashion) and the mapping procedure was repeated for each such structure derived. The location of the most stereoinducing region was invariant to twists up to 15 degrees. Small variations in actual transition-state geometry are not expected to change the results described in this paper. Similarly, we found that our results are relatively insensitive to atom-centered charges assigned to both the probes and the catalyst when realistic dielectric constants are used. Finally, we are cognizant of the fact that a myriad of other influencing factors such as solvation, temperature, and so forth will influence the stereochemical outcome of these reactions; these influences have been omitted in this study. Our goal here is to strip the system to its bare essentials, confirm or deny the proposed hypothesis, and to provide a simple computational protocol for the scientific community to use when designing new catalysts.

Computational Tools. All quantum chemical calculations were done using Spartan 5.0.[5] The PM3(tm) Hamiltonian was used which implements Wavefunction's transition-metal parameter set.[5] Transition-state searches and geometry optimizations were carried out using default convergence criteria. Atomic charges were assigned using the electrostatic fitting routines in Spartan. Conformational analyses were done using grid searching with Spartan. Placement of catalyst into a 3-D grid and other manipulations such as superimposing structures were done using MacroModel 7.0.[6] The energy calculations were done using an in-house program called mmod-grid that has been parallelized with Parallel Virtual Machine (PVM). The parallelized program was

(3) Kanemasa, S.; Oderaotashi, Y.; Yamamoto, H.; Tanaka, J.; Wada, E.; Curran, D. P. *J. Org. Chem.* **1997**, *62*, 6454−6455.
(4) Cambridge Structural Database: Available from Wavefunction, Inc., 18401 Von Karman, Suite 370, Irvine, CA 92715.
(5) Spartan: Available from Wavefunction, Inc., 18401 Von Karman, Suite 370, Irvine, CA 92715.
(6) Mohamadi, F.; Richards, N. G. J.; Guida, W. C.; Liskamp, R.; Lipton, M.; Caufield, C.; Chang, G.; Hendrickson, T.; Still, W. C. *J. Comput. Chem.* **1990**, *11*, 440−467.

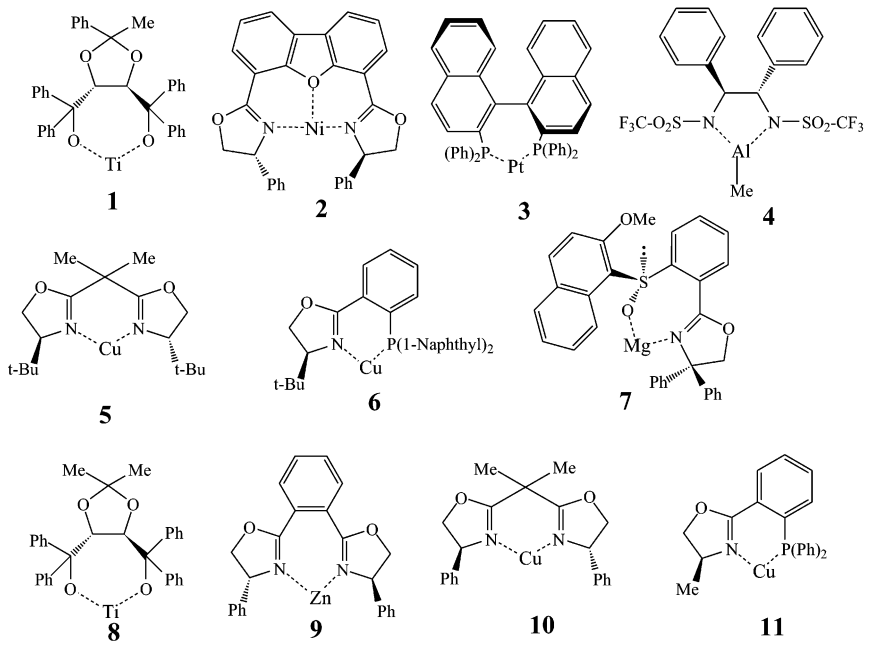

Figure 5. Chiral catalysts used to induce asymmetry during the Diels−Alder reaction of 3-acryloyl-2-oxazolidin-2-one and cyclopentadiene that are part of this study. Catalysts **1**−**7** are efficient but catalysts **8**−**11** are not.

designated as pvm-grid.[7] This program is written in C and is available free of charge from the authors. The calculations described in this paper were done using a loosely networked cluster of SGI machines and on a small cluster of 26 AMD Athlon processors running a Linux operating system (more information about this will appear in the Ph.D. thesis of JS). The dimensions of the grid surrounding the catalyst are such that the sampling region is at least 5 Å beyond the catalyst in the *x*, *y*, and *z* direction; accordingly, the sampling box varies in size from catalyst to catalyst. The grid spacing is set to 0.25 Å and at each grid point the transition-state probe is rotated in 30° increments about the *x*, *y*, and *z* axes, giving rise to 1728 intermolecular calculations at each grid point that are then Boltzmann averaged. A typical run consists of a cubic 17 Å sampling box containing ∼275,000 grid points; the number of configurations involved is thus about 475 million for the R probe and an equivalent number for the S probe. The force field used in these calculations is AMBER*.[8] No cutoffs of any kind were implemented in the grid calculations. The dielectric constant used in the energy calculations is set to the dielectric of the medium in which the reactions were carried out experimentally. Visualization of the results is done with NAG's IRIS Explorer 4.0.[9]

Systems Studied. Because this is a preliminary study on the topic of stereocartography, we looked for systems fulfilling the following requirements: (1) The publication from which we extracted our information should have a complete assessment of reaction conditions such that the reported ee is deemed reliable; the efficacy of many catalyzed reactions is often found to be dependent upon more than just the ligand used. In particular, the metal (including its spin and oxidation state), the solvent, the temperature, and the nature of the counterions associated with the catalyst before substrate binding all impact the observed stereochemisty. The systems we selected are all well studied in this regard by the authors who created each catalyst. The ee's used in our analyses are thus considered to be the maximum values corresponding to the optimum reaction conditions for a given ligand. (2) The reaction taking place should be as simple as possible. In the examples described below, we select Diels−Alder reactions because the transition state for this concerted pericyclic reaction is relatively easy to derive computationally. (3) The catalyst ligands should contain as few conformational degrees of freedom as possible. We opt for systems containing phenyl, methyl, *tert*-butyl, and similar substituents appended to the ligand so that no ambiguity exists about the structure of the catalyst; in some instances more than a single conformation of isopropyl and other stereodirecting substituents are accounted for as described above.

Scheme 1

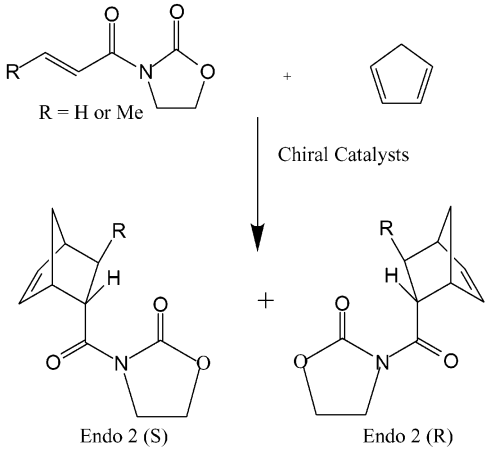

Next, while we are interested in studying why highly effective catalysts work as they do, we are also obliged to understand why poorly performing catalysts are inefficient. In this work, we designate "efficient" catalysts as those giving ee's in excess of 70% (most studied here are in excess of 90%) and "inefficient" catalysts as having ee's under 60%. The first reaction to be described below is the Lewis acid catalyzed cycloaddition of 3-acryloyl-1,3-oxazolidin-2-one with cyclopentadiene depicted in Scheme 1. In this reaction, both *exo* and *endo* stereoisomers are produced with the *endo* adduct being the dominant product. The reaction is carried to fruition efficiently by catalysts **1**−**7**, but they are inefficiently catalyzed by **8**−**11** (Figure 5). Note the

(7) pvm_grid is a suite of programs written by Bob Coner. It allows one to compute intermolecular interactions between a host and a guest molecule with several different force fields and contains a variety of analysis tools. Input files are MacroModel format.[6] To maximize usage of existing and remote machines, pvm_grid is parallelized using the PVM (Parallel Virtual Machine) Library (http://www.epm.ornl.gov/pvm/pvm_home.html).

(8) AMBER* is a modified version of the AMBER force field contained in MacroModel.

(9) Numerical algorithms Group, IRIS Explorer. IRIS Explorer Center (North America), Downers Grove, IL 60551-5702 or via http://www.nag.co.uk/Welcome_IEC.html.

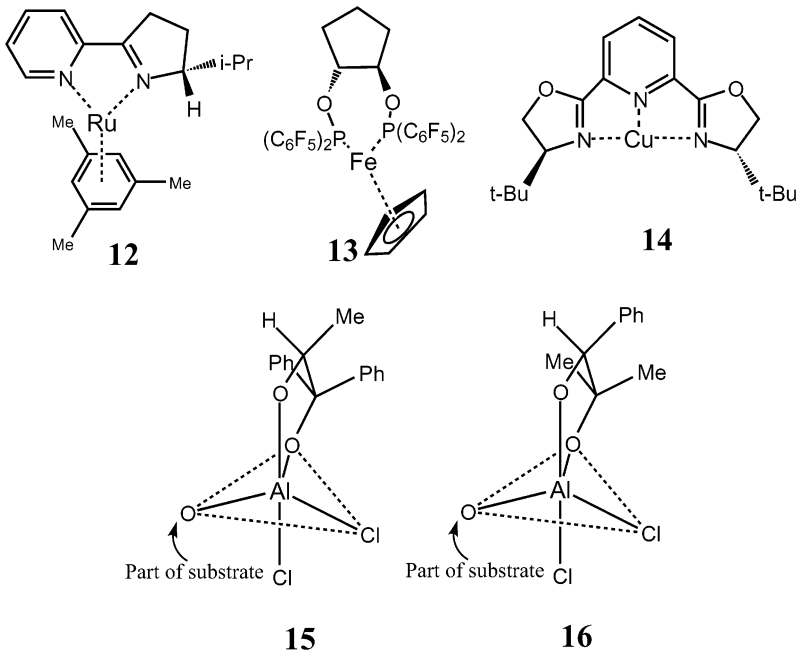

Figure 6. Chiral catalysts used in this study that catalyzed the Diels−Alder reaction of cyclopentadiene with acrolein dienophiles. Catalysts **12**−**15** are efficient at stereoinduction but catalyst **16** is not.

Scheme 2

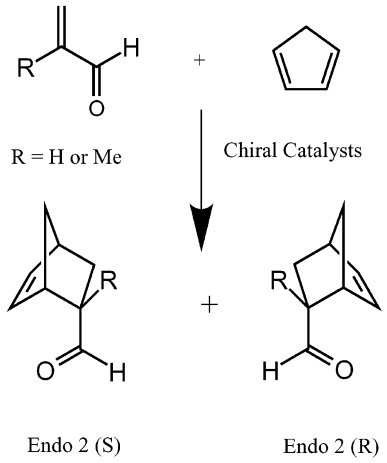

Scheme 3

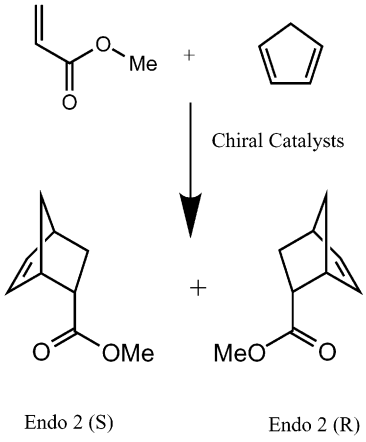

structural relationships between **5** (an efficient catalyst) and **10** (an inefficient one). Likewise note the relationships between **6** and **11** as well as **1** and **8**. It will be shown below that the regions of maximum stereoinduction are near the site of chemistry for the good catalysts but not for the ineffective catalysts despite the similarity in structure.

The second reaction we evaluated is the cycloaddition of acroleins to cyclopentadiene depicted in Scheme 2. Again, *exo* and *endo* products are obtained with *endo* being the dominant product. The efficient catalysts for this reaction are **12**−**15** whereas the inefficient catalyst is **16** depicted in Figure 6. The final reaction scheme we evaluated is the cycloaddition of cyclopentadiene with methylacrylate (Scheme 3). Catalyst **17** is an efficient catalyst while catalyst **18** is not (Figure 7).

Results

Catalyst 1. Narasaka et al.[10] examined the Diels−Alder reaction of 3-crotonoyloxazolidinone with cyclopentadiene using dichlorotitanium alkoxides derived from various chiral diols. These researchers started with a marginally effective chiral Lewis acid catalyst (2R,3R)-2,3-O-isopropylidine-1,1,4,4-tetraphenyl-1,2,3,4-butanetetrol·$TiCl_2$ (catalyst **8** in Figure 5) and optimized the system to a very effective chiral Lewis acid catalyst (2R,3R)-2,3-O-(1-phenylethylidene)-1,1,4,4-tetraphenyl-1,2,3,4-butanetetrol·$TiCl_2$ (catalyst **1** in Figure 5). Enantioselectivity was found to depend strongly on the acetal substituents.[10] Catalyst **1** had the optimal enantioselectivity of all the acetal substituent variations considered by those researchers. Catalyst **8** had a marginal enantioselectivity even though the difference between **1** and **8** is only a single acetal substituent modification as shown in Figure 5. A crystal structure of catalyst **8** was retrieved from the CSD (refcode YUGJAL).[11] The isopropylidene acetal substituent was changed to a 1-phenylethylidene substituent to create catalyst **1** and the structure was geometry optimized using the PM3(tm) Hamiltonian. Chlorine counterions, which were retained only for computing structures and charge distributions, were removed for the grid calculations. The reaction was run in toluene ($\epsilon = 2.38$) and, accordingly,

(10) Narasaka, K.; Iwasawa, N.; Inoue, M.; Yamada, T.; Nakashima, M.; Sugimori, J. *J. Am. Chem. Soc.* **1989**, *111*, 5340−5345.

(11) Seebach, D.; Plattner, D. A.; Beck, A. K.; Wang, Y. M.; Hunziker, D.; Petter, W. *Helv. Chim. Acta* **1992**, *75*, 2171−2192.

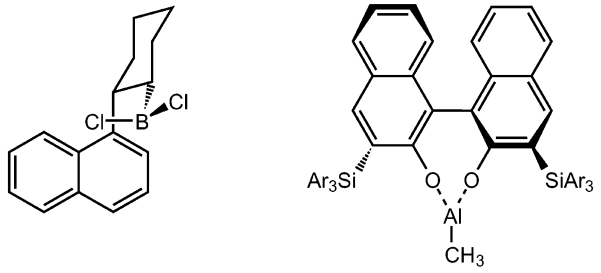

17 18

Figure 7. Two catalysts used in this study. One catalyst (**17**) is effective at inducing asymmetry during the Diels−Alder reaction of cyclopentadiene with methylacrylate but the other is not.

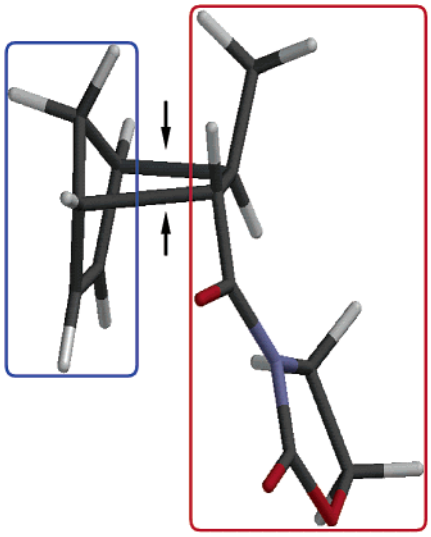

Figure 8. A computed transition state between cyclopentadiene and 3-acryloyl-2-oxazolidin-2-one. The diene is encircled in blue, the dienophile encircled in red, and the arrows are pointing to the nascent bonds.

our dielectric was set to this value for the grid calculations. The transition-state probe used in these calculations is depicted in Figure 8.

The mirror image of this transition state was generated by reflection of coordinates through the *xy* plane and these enantiomeric transition-state probes were then used in the grid calculations.

The result for catalyst **1** is shown in Figure 9. The most significant result is that the region of maximum stereoinduction for this efficient catalyst is congruent with the site of chemistry. The distance between the site of maximum stereoinduction and the oxazolidin-2-one/cyclopentadiene transition-state nitrogen atom is 1.57 Å. For this catalyst, our hypothesis is proved correct.

Catalyst 2. Yamamoto et al.[12] studied a highly effective chiral Lewis acid catalyst, (R,R)-4,6-dibenzofurandiyl-2,2′-bis(4-phenyloxazolidine)·$Ni(ClO_4)_2$·$3H_2O$. Several metal perchlorates complexed with (R,R)-4,6-dibenzofurandiyl-2,2′-bis(4-phenyloxazoline) show high catalytic and enantioselective activity in the Diels−Alder reaction of cyclopentadiene with 3-acryloyl-1,3-oxazolidin-2-one. Nickel perchlorate had the optimal combination of time, yield, *endo*:*exo* ratio, and enantiomeric excess. The reactions were run in dichloromethane with varying amounts of water, with no variations in enantioselectivity. The major product from this reaction is the *endo* (R) enantiomer. In a later paper,[13] Yamamoto confirmed with X-ray crystallography that the catalyst-dienophile complex is square bipyrimidal with an octahedral nickel ion. The X-ray structure of **2** was taken directly from the Cambridge Structural Database (CSD refcode NOVBAB). The X-ray structure contained ClO_4 counterions that were retained only for computing charge distributions. The counterions were then removed for the grid calculations.

The catalyst was placed in a uniform grid and the two Diels−Alder transition-state probes were used to sample and statistically weight the interaction energies at each grid point. Difference plots were then generated to locate the region of maximum stereoinduction for the favored (R) product. The result for catalyst **2** is shown in Figure 10.

The top row of frames again illustrates only the docked transition-state structure for this catalyst. The bottom row of frames shows the most enantiodiscriminating region encapsulated within a sphere of 1 Å radius (centered about the most enantiodiscriminating grid point). What is significant in this figure is the distance from the sphere to the transition-state probe. In this example, they are close to one another with the distance from the most stereoinducing grid point to the oxazolidin-2-one/cyclopentadiene transition-state nitrogen being 1.92 Å, a result that is consistent with the working hypothesis.

Catalyst 3. Ghosh et al.[14] studied a highly effective chiral Lewis acid catalyst, (2,2′-bis(diphenylphosphino)-1,1′-binaphthyl-P,P′)-platinum(II)·$(SbF_6)_2$. Ghosh found **3** to be a highly effective chiral catalyst for the Diels−Alder reaction of 3-acryloyl-1,3-oxazolidin-2-one with cyclopentadiene while run in dichloromethane at −78 °C. Several counterions complexed with (2,2′-bis(diphenylphosphino)-1,1′-binaphthyl-P,P′)-platinum-(II) show high catalytic and enantioselective activity with this reaction. Hexafluoroantimony counterion afforded superior *endo* enantioselectivity and a nearly quantitative isolated yield. Ghosh hypothesizes that platinum(II) adopts a square-planar geometry with the ligand and the bidentate acyl oxazolidinone substrate. Using **3** as the catalyst, the major cycloaddition product is the *endo* (S) enantiomer. Catalyst **3** was generated by us from an X-ray structure in the CSD containing a similar transition metal bound to the same chiral ligand. (η^6-Benzene)-chloro-(2,2′-bis-(diphenylphosphino)-1,1′-binaphthyl-P,P′)·ruthenium (II) (CSD refcode JAPZAL) served as the progenitor to **3**. The ruthenium-(II) was changed to a platinum(II) and the structure was geometry optimized using the PM3(tm) Hamiltonian. The results are presented in figure S11 (see Supporting Information) where it is noted that the region of maximum stereoinduction for this catalyst is spatially congruent with the site of chemistry.

Catalyst 4. Corey et al.[15] prepared (3S,4S)-2,5-bis(trifluoromethylsulfonyl)-1-alumina-2,5-diazacyclopentane, catalyst **4**, and found it to be efficient for the cycloaddition of cyclopentadiene with 3-acryloyl-1,3-oxazolidin-2-one at low temperatures in dichloromethane. In a following paper,[16] Corey confirmed with NMR data monocoordination of the dieneophile to the

(12) Kanemasa, S.; Oderatoshi, Y.; Yamamoto, H.; Tanaka, J.; Wada, E. *J. Org. Chem.* **1997**, *62*, 6454−6455.

(13) Kanemasa, S.; Oderaotoshi, Y.; Sakaguchi, S.; Yamamoto, H.; Tanaka, J.; Wada, E.; Curran, D. P. *J. Am. Chem. Soc.* **1998**, *120*, 3074−3088.
(14) Ghosh, A. K.; Matsuda, H. *Org. Lett.* **1999**, *1*, 2157−2159.
(15) Corey, E. J.; Imwinkelried, R.; Pikul, S.; Xiang, Y. B. *J. Am. Chem. Soc.* **1989**, *111*, 5493−5495.
(16) Corey, E. J.; Sashar, S. *J. Am. Chem. Soc.* **1992**, *114*, 7938−7939.

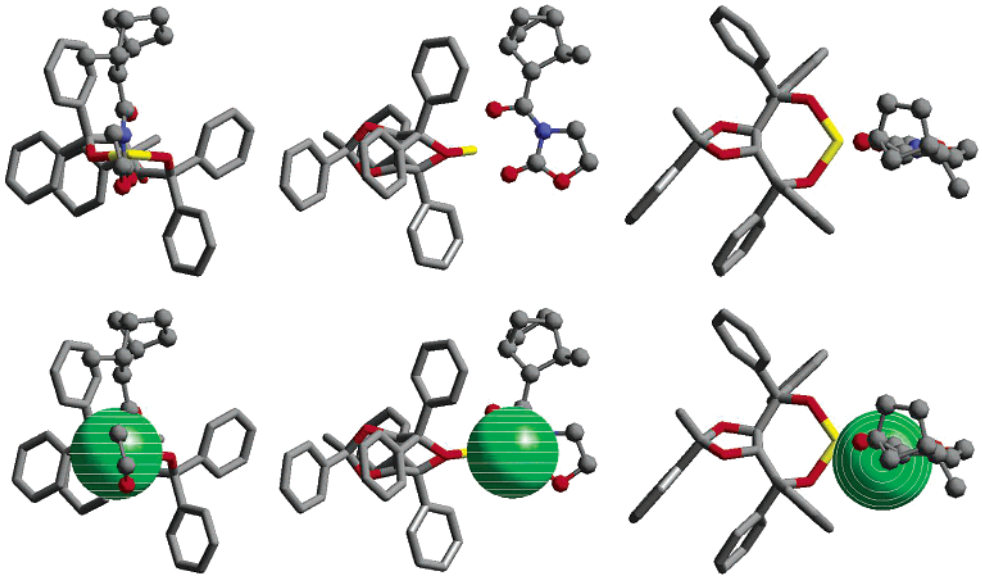

Figure 9. Location of transition-state probe and region of maximum stereoinduction for catalyst **1**. The frames in the columns from left to right show, respectively, front, side, and top views of the docked transition state with the catalyst. In all frames, the catalyst is depicted in a cylinder (tube) format while the transition-state probe is shown in a ball-and-stick format. All hydrogen atoms have been removed for clarity. The top row of frames illustrates only the docked transition-state structure for this catalyst system. The bottom row shows the most enantiodiscriminating region encapsulated within a sphere of 1 Å radius (centered about the most enantiodiscriminating grid point).

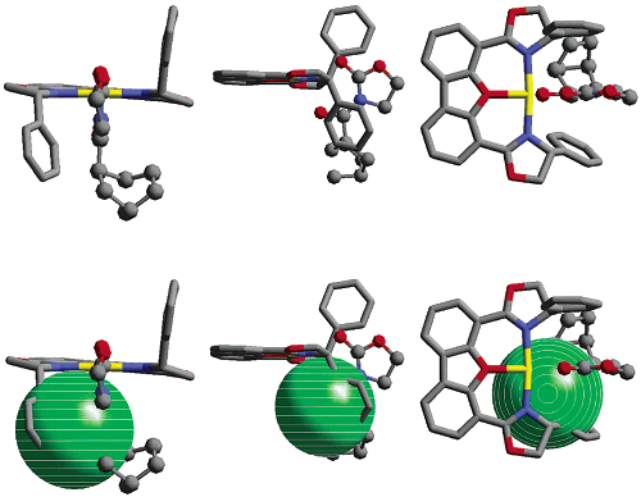

Figure 10. Location of transition-state probe and region of maximum stereoinduction for catalyst **2**. See caption of Figure 9 for details concerning the graphic.

aluminum. A dimeric crystal structure 1,5-bis(trifluoromethyl)-3,7-dimethyl-1,5-dioxo-(2,3:6,7-(1S,2S)bis(1,2)-diphenyl-3-trifluormethylsulfonyl)-3-azapropano-1,5-dithia-2,6-diaza-3,7-dialumina-4,8-dio xacyclooctane (CSD refcode VUTLEB) was used to generate the structure of catalyst **4** for the mapping process. Two conformers were obtained within 1.5 kcal/mol of one another and both were used in the mapping protocol. The lower energy structure has the trifluoromethyl groups parallel to the mean plane of the five-member metallo-cyclopentane while the higher energy structure has the groups normal to this plane. Both conformers were used in the analysis. The results are presented in Figure 12. In this figure, there are superimposed two conformations of the catalyst, each with its associated transition state. The midpoint between the two nitrogen atoms of the 3-acryloyl-1,3-oxazolidin-2-one moiety of these transition states was used to define the "site of chemistry". There exists only one site of maximum stereoinduction because the grid points have already been Boltzmann weighted to account for both conformers of catalyst. The distance between the site of chemistry and the grid point of maximum stereoinduction is 1.33 Å. Hence, this catalyst has its most stereoinducing region at the site of chemistry and is consonant with the working hypothesis.

Catalyst 5. Previous work by Evans et al.[17] demonstrated the excellent utility of C_2-symmetric bis(oxazoline)-derived Cu(I) and Cu(II) complexes for enantioselective group transfer processes such as cyclopropanation and aziridination. These researchers also proved Cu(II) complexes as being effective chiral Lewis acid catalysts in Diels−Alder cycloaddition reactions of imide dienophiles with cyclopentadiene. Evans started with a poor chiral catalyst (4S,4S)-(bis(phenyloxazolin-2-yl)-methane)-bis(trifluoromethylsulfonate)-copper(II) (catalyst **9** which will be described later in this paper) and optimized it to (4S,4S)-(bis(4-*tert*-butyloxazolin-2-yl)methane)-bis(hexafluoroantimonate)-copper (II) (catalyst **5**) which is excellent for the Diels−Alder reaction of 3-acryloyl-1,3-oxazolidin-2-one with cyclopentadiene. Evans expected the bidentate dienophile to easily replace the triflate counterions. In earlier work, he studied several counterions under the same reaction conditions and found hexafluoroantimonate counterions to display greatly enhanced catalytic efficiency.[18] Evans then compared triflate and hexafluoroantimonate counterions at various reaction temperatures and found hexafluoroantimonate to be the optimal counterion for asymmetric catalysis. He proposes a four-coordinate square-planar bis(oxazoline)·Cu(II)·dienophile complex, with *s-cis* dienophile geometry as the structure that will

(17) (a) Evans, D. A.; Woerpel, K. A.; Hinman, M. M.; Faul, M. M. *J. Am. Chem. Soc.* **1991**, *113*, 726−728. (b) Lowenthal, R. E.; Abiko, A.; Masamune, S. *Tetrahedron Lett.* **1990**, *31*, 6005−6008. (c) Müller, D.; Umbricht, B. W.; Pfaltz, A. *Helv. Chim. Acta* **1991**, *74*, 232−240. (d) Evans, D. A.; Faul, M. M.; Bilodeau, M. T.; Anderson, B. A.; Barnes, D. M. *J. Am. Chem. Soc.* **1993**, *115*, 726−728. (e) Evans, D. A.; Faul, M. M.; Bilodeau, M. T. *J. Am. Chem. Soc.* **1994**, *116*, 2742−2753.

(18) Evans, D. A.; Miller, S. J.; Lectka, T.; von Matt, P. *J. Am. Chem. Soc.* **1999**, *121*, 7559−7573.

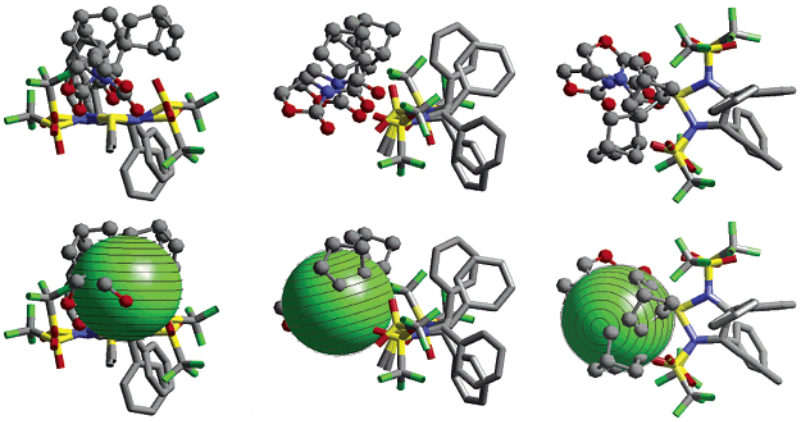

Figure 12. Location of transition-state probe and region of maximum stereoinduction for catalyst **4**. See caption of Figure 9 for details concerning the graphic. In the diagram, two conformational states of the catalyst along with two transition-state probes are depicted.

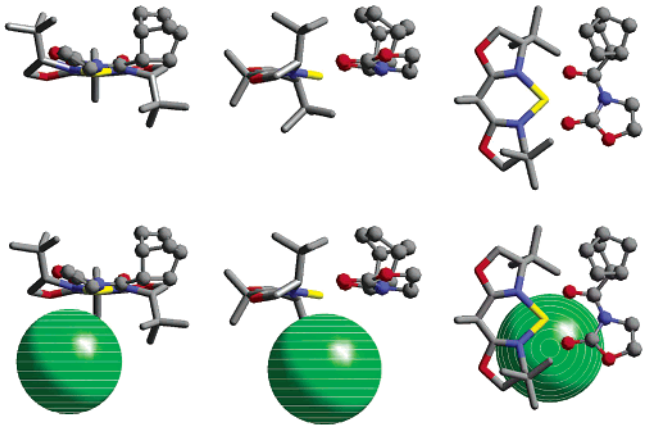

Figure 13. Location of transition-state probe and region of maximum stereoinduction for catalyst **5**. See caption of Figure 9 for details concerning the graphic.

undergo attack by the diene. Using **5** as the catalyst, the major product is the *endo* (S) enantiomer.

The catalyst **5** was taken from an X-ray structure found in the CSD (refcode GIWHID). (4S,4S)-(Bis(4-*tert*-butyloxazolin-2-yl)methane)-diaqua-(trifluoromethylsulfonato- O)·copper(II)·(trifluoromethylsulfonate) was the structure that served as the progenitor to **5** (we removed the waters and the triflate counterions for the grid calculations). The results show (Figure 13) that the region of greatest enantioinduction is not congruent with the site of chemistry. The distance between the site of maximum stereoinduction and the oxazolidin-2-one/cyclopentadiene transition-state nitrogen atom is 4.89 Å. For this catalyst, our hypothesis is proved incorrect. This is the only example from our studies where our hypothesis is not validated. Possible reasons for this will be described later in the paper.

Catalyst 6. Helmchen et al.[19] sought to enhance Lewis acidity to copper(II) by using a phosphorus σ-donor/π-acceptor ligand compared to the nitrogen-donor ligands Evans[20] discovered. Helmchen found (4S)-(2-(2-bis(1-naphthyl)-phosphinophenyl)-4-(*tert*-butyl)-oxazoline)·copper(II)·(OTf)$_2$ to be an excellent chiral catalyst (catalyst **6**) for the Diels−Alder reaction of 3-acryloyl-1,3-oxazolidin-2-one with cyclopentadiene. Enantioselectivity was found to depend strongly on the size of both the substituent on the oxazoline ring and the P−Ar group of the chiral ligand.[19] Copper(II) complexes with less bulky aryl groups at phosphorus and on the oxazoline ring provided lower selectivity. Using **6**, the Diels−Alder reaction was run in dichloromethane and accordingly the dielectric of the grid medium was set to $\epsilon = 8.9$. OTf counterions provided slightly better enantioselectivity than SbF_6, but the reaction with SbF_6 counterions was faster. Helmchen proposes a square-planar phosphorus-oxazolidine·Cu(II)·dienophile complex, similar to Evans.[20] Using **6** as the catalyst, the major product is the *endo* (S) enantiomer.

Catalyst **6** was generated from an X-ray structure in the CSD containing a similar chiral ligand (CSD refcode LELKAO). (4S)-(2-(2-((1-Naphthyl)-phenylphosphino)phenyl)-4-(2-propyl)-oxazolidine)-(η^3 -propenyl)·palladium(II)·$(SbF_6)_2$ served as the progenitor to **6**. We removed the η^3-propenyl and square-planar copper(II) was used to replace palladium(II). The isopropyl substituent was changed to a tertiary butyl substituent and the phenyl substituent was changed to a second 1-naphthyl substituent. The SbF_6 counterions were replaced by chelating OTf counterions that were retained only for geometry optimization and computing charge distributions. The OTf ions were removed for the grid calculations. The results are presented in figure S14 (see Supporting Information). Again, we point out that what is significant is the distance from the sphere to the transition-state probe; the distance between the site of chemistry and the region of maximum stereoinduction is 2.19 Å which is consistent with our hypothesis.

Catalyst 7. Hiroi has recently developed a set of chiral sulfoxide ligands coordinated to magnesium for catalytic asymmetric Diels−Alder reactions of 3-acryloyl-1,3-oxazolidin-2-one with cyclopentadiene.[21] One of the effective catalysts depicted in Figure 5 is **7**. A somewhat more efficient catalyst exists in Hiroi's paper but was not selected for study here because it contains a 2-methoxyisopropyl substituent making it too conformationally complex for our needs. The *endo*-2-(S) product is formed as the major product when carried out in dichloromethane. This catalyst was constructed de novo with two I atoms coordinated to the Mg. The seven-member ring containing the metal can assume one of two boatlike puckered forms, one of which is significantly more stable than the other.

(19) Helmchen, G.; Sagasser, I. *Tetrahedron Lett.* **1998**, *39*, 261−264.
(20) (a) Evans, D. A.; Miller, S. J.; Lectka, T. *J. Am. Chem. Soc.* **1993**, *115*, 6460−6461. (b) Evans, D. A.; Lectka, T.; Miller, S. J. *Tetrahedron Lett.* **1993**, *34*, 7027−7030. (c) Dias, L. C. *J. Braz. Chem. Soc.* **1997,** *8* (4), 289−332. (d) Hoveyda, A. H.; Morken, J. P. *Angew. Chem., Int. Ed. Engl.* **1996**, *35*, 1262−1284.
(21) Hori, K.; Watanabe, K.; Abe, I.; Michiko. K. *Tetrahedron Lett.* **2001**, *42*, 7617−7619.

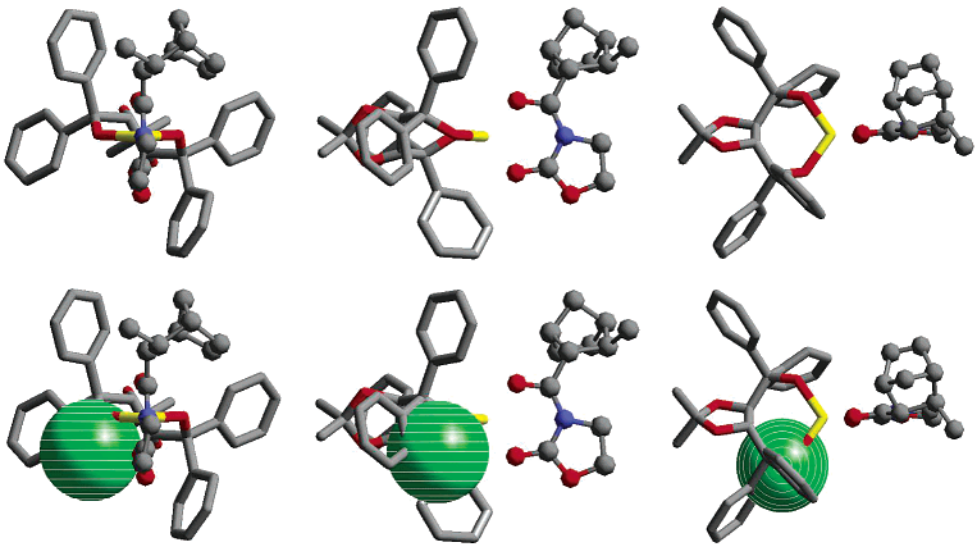

Figure 16. Location of transition-state probe and region of maximum stereoinduction for catalyst **8**. See caption of Figure 9 for details concerning the graphic.

A conformational analysis of the favorable puckered system revealed two conformations, within one kcal/mol of one another, that were used in our analysis. These conformers differ only in the orientation of the 2-methoxy-1-naphthyl group; one conformer has the methoxy-bearing ring above the metallocycle while the other has it below that ring. The iodines were removed and the corresponding enantiomeric transition states were used to sample the interaction energies as before. Difference plots located the region of maximum stereoinduction that is encased in a green sphere in figure S15 (see Supporting Information). In this figure, two catalyst conformers and two bound transition-state probes corresponding to those two conformers exist. Again, consistent with the working hypothesis, there is a spatial congruence between the site of chemical reaction and the site of maximum stereoinduction.

Catalyst 8. We mentioned earlier that Narasaka et al.[10] examined the Diels−Alder reaction of 3-crotonoyloxazolidinone with cyclopentadiene using dichlorotitanium alkoxides derived from various chiral diols. Narasaka started with a marginally effective chiral Lewis acid catalyst, (2R,3R)-2,3-O-isopropylidine-1,1,4,4-tetraphenyl-1,2,3,4-butanetetrol·($TiCl_2$). We are interested in this ligand because of its poor performance. We found the X-ray structure of **8** in the CSD (refcode JUPWAS). Chlorine counterions, which were retained only for computing charge distributions, were removed for the grid calculations. The results are presented in Figure 16 and show that the region of maximum enantioinduction is not congruent with the site of chemistry. The site of chemistry is close to the transition metal, in "front" of the catalyst and between the phenyl groups. The region of maximum enantioinduction is not in "front" of the metal center and it does not overlap with the site of chemistry. The distance between the site of maximum stereoinduction and the oxazolidin-2-one/cyclopentadiene transition-state nitrogen atom is 5.33 Å, a distance well removed from the site of chemistry.

Catalyst **8** is not an effective enantioselective system for this reaction. For catalyst **8**, the region of maximum enantioinduction is indeed far from the theoretical site of chemistry. Narasaka's group eventually optimized **8** to **1**, a highly effective Lewis acid system, whose aforementioned regions are spatially coincident; for this pair of catalysts, then, our hypothesis is proved correct even though a small structural modification was made.

Catalyst 9. Tackas et al.[22] were interested in room-temperature Lewis acid catalyzed Diels−Alder cycloaddition reactions of N-crotonyloxazolidine with cyclopentadiene. Takacs sought to make a better catalyst by using a highly constrained chiral ligand but found (1,2-bis((4S)-4-phenyl-2-oxazolin-2-yl)benzene)·zinc(II) to have poor enantioselectivity for this Diels−Alder reaction. For our work, catalyst **9** was generated from an X-ray structure containing a similar chiral ligand (CSD refcode KISMOO). Dichloro-(1,2-bis((4S)-4-isopropyl-2-oxazolin-2-yl)-benzene)·zinc(II) is the CSD X-ray structure that served as the progenitor to **9**. The isopropyl groups were changed to phenyl groups and the chlorine counterions, which were retained only for computing charge distributions, were removed for the grid calculations. The stereocartography results are shown in figure S17 where it is clear that the spatial congruence needed for a catalyst to be effective is missing. Indeed, the distance between the site of chemistry and the region of maximum stereoinduction is 6.98 Å.

Catalyst 10. This catalyst is inefficient at chirality transfer for the Diels−Alder reaction of 3-acryloyl-1,3-oxazolidin-2-one with cyclopentadiene The background for this catalyst was described earlier where we pointed out that Evans started his studies initially with several ineffective chiral catalysts, including (4S,4S)-(bis(phenyloxazolin-2-yl)methane)-bis(trifluoromethylsulfonate)-copper(II) to promote this reaction. These are poor catalysts that were eventually modified by replacing the phenyl substituents on the oxazoline rings with *tert*-butyl groups (catalyst **5**) but we consider catalyst **10** in our study because it is deemed to be an ineffective catalyst. As such, it ought not to have spatial congruence between the region of maximum stereoinduction and the site of chemistry and, as shown in figure S18 (Supporting Information), this expectation is confirmed. The structure used for catalyst **5** was used here but with the *tert*-butyl groups replaced with phenyl groups. The same

(22) Takacs, J. M.; Quincy, D. A.; Shay, W.; Jones, B. E.; Ross, C. R.; *Tetrahedron: Asymmetry* **1997**, *8*, 3079−3087.

dielectric constant was used here as in **5**. The distance between the site of chemistry and the region of maximum stereoinduction is 4.32 Å.

Catalyst 11. As mentioned in a previous section, Helmchen et al.[19] started with (4S)-(2-(2-diphenylphosphinophenyl)-4-(methyl)-oxazolidine)·copper(II)·$(OTf)_2$ but found it to have poor enantioselectivity for the Diels−Alder reaction of 3-acryloyl-1,3-oxazolidin-2-one with cyclopentadiene. This is an especially interesting system to study because it contrasts with the highly efficient catalyst **6**. Catalyst **11** was generated from an X-ray structure in the CSD (refcode LELKES). (4S)-2-(2-(Diphenylphosphinophenyl)-4-(2-propyl)-oxazoline)-(η^3-1,3-diphenylpr openyl)·palladium(II)·$(SbF_6)_2$ served as the progenitor to **11**. We removed the η^3-1,3-diphenylpropenyl group and a square-planar copper(II) was used to replace palladium(II). The isopropyl substituent was changed to a methyl substituent. The SbF_6 counterions were replaced by OTf counterions that were retained only for geometry optimization and computing charge distributions. The OTf ions were removed for the grid calculations. After those structural modifications, we geometry optimized **11** using the PM3(tm) Hamiltonian. The same dielectric constant used for catalyst **6** was used for catalyst **11** in the mapping process. The results are presented in figure S19 (Supporting Information) where one clearly finds no spatial congruence between the site of chemistry and the region of maximum stereoinduction. Indeed, the distance between these sites is 9.47 Å (compare this result with the 2.19 Å distance found in catalyst **6**). Hence, this inefficient catalyst conforms to our working hypothesis.

Catalyst 12. We begin this section by pointing out that this and the following four catalysts involve a different cycloaddition reaction than those described above (see Scheme 2). The dienophile in these examples is methacrolein. In contrast to 3-acryloyl-1,3-oxazolidin-2-one described above, which can bind to the metal center in a bidentate manner, this dienophile can associate only in a monocoordinate manner through the acrolein carbonyl. The cycloaddition transition state for this reaction is presented in figure S20 (Supporting Information) with the diene encircled in blue, the dienophile encircled in red, and arrows pointing to the forming bonds. The mirror image of this transition state was generated by reflection of coordinates through the *xy* plane and these enantiomeric transition states were then used in the grid calculations.

The first use of half-sandwich arene ruthenium complexes with bisoxazoline ligands as chiral Lewis acid catalysts was reported in 1996.[23] The following year Davies et al.[24] studied an effective chiral Lewis acid catalyst, aqua-bis(hexafluoroantimony)-4-isopropyl-2-(2-pyridyl)-(1,3-oxazolin-2-yl)-(η^6- mesityl)-ruthenium, for the Diels−Alder reaction of methacrolein with cyclopentadiene. Davies' group assumes that the methacrolein coordinates in the preferred *s-trans* conformation, with the aldehyde hydrogen pointing toward the arene ring. The alternative orientation obtained by a 180° rotation about the Ru−O bond would be disfavored because of steric interactions between the methyl substituent and the arene. The *si* face of the dienophile is shielded by the isopropyl substituent of the chiral ligand that is consistent with the experimentally observed *exo* (S), product. Catalyst **12** was generated from an X-ray structure in the CSD, chloro-(4-isopropyl-2-(2-pyridyl)-1,3-oxazolin-2-yl)-(η^6-mesityl)-ruthenium (CSD refcode NIGMUL). No conformational analysis was carried out. The results are presented in figure S21 (Supporting Information) where one finds the site of chemistry and the region of maximum stereoinduction to be spatially congruent (distance = 0.78 Å).

Catalyst 13. Kündig et al.[25] studied an effective chiral Lewis acid catalyst, (η^5-cyclopentadienyl)-*trans*-(1R,2R)-1,2-cyclopentanediyl-bis((bis(pentafluorophe nyl)-phosphinoxy)-P,P′)-Fe-(BF_4), catalyst **13**. Catalyst **13** showed catalytic and enantioselective activity in several cycloaddition reactions of a, b substituted acroleins, including methacrolein, with cyclopentadiene. On the basis of the crystal structure of a very similar chiral ligand, Kündig proposed an intermediate complex structure of **13**·methacrolein that accounts for the observed stereoselectivity. Methacrolein favors the *s-trans* conformer and this preference is enhanced upon complexation to a Lewis acid.[26] Steric hindrance between the methyl substituent of the substrate and the η^5-cyclopentadienyl substituent of **13** provides a structure such that the *re* face is shielded by a pentafluorophenyl ring of **13**'s chiral ligand. Catalyst **13** was generated from an X-ray structure in the CSD, (η^5-cyclopentadienyl)-acetonitrile-*trans*-1,2-cyclopentadienyl-bis-((bis(pentafluoro phenyl)phosphinoxy)-P,P′)-Fe, (CSD refcode HETYAG). For our work, we removed the cocrystallized acetonitrile. The X-ray structure contained hexafluorophosphate counterions that were retained only for computing charge distributions. The counterions were then removed for the grid calculation. The results are presented in figure S22 (Supporting Information) where again there is a spatial congruence of the regions of interest.

Catalyst 14. Evans et al.[27] prepared a copper(II) complex with a tridentate bis(oxazolinyl) pyridine ligand in an effort to broaden the utility of Lewis acid chiral Cu(II) complexes. Evans anticipated the formation of a square-planar coordination geometry around the copper transition metal, leaving a single coordination site for substrate. It was discovered that counterion effects strongly influence the reactivity of tridentate bis-(oxazolinyl) pyridine ligand complexes and he found the [Cu^{II}-(pybox)(SbF_6)] complex to be an effective chiral Lewis acid for the cycloaddition of methacrolein with cyclopentadiene. CSD refcode CEBQAB resembles closely the desired catalyst. CEBQAB contains SbF_6 counterions but it has isopropyl substituents instead of tertiary butyl substituents. The isopropyl substituents were modified to tertiary butyl groups and the SbF_6 counterions were retained only for computing charge distributions. The results of our calculations are presented in Figure 23 where the region of maximum stereoinduction and the site of chemistry are separated by 1.18 Å. Hence, this catalyst and the others described above support the hypothesis presented.

Catalysts 15 and 16. Kagan et al.[28] sought an effective chiral Lewis acid catalyst to elaborate upon the pioneering work of

(23) Asano, H.; Katayama, K.; Kurosawa, H. *Inorg. Chem.* **1996**, *35*, 5760−5761.
(24) Davies, D. L.; Fawcett, J.; Garratt, S. A.; Russell, D. R. *J. Chem. Soc., Chem. Commun.* **1997**, 1351−1352.
(25) Kündig, E. P.; Bourdin, B.; Bernardinelli, G. *Angew. Chem., Int. Ed. Engl.* **1994**, *33*, 1856−1858.
(26) Yamamoto, H.; Pfaltz, A.; Jacobsen, E. N. In *Comprehensive Asymmetric Catalysis*; Jacobsen, E. N., Pfaltz, A., Yamamoto, H., Eds.; Springer: Berlin, **1999**; Vol. 3, pp 1181−1182.
(27) Evans, D. A.; Murry, J. A.; von Matt, P.; Norcross, R. D.; Miller, S. J. *Angew. Chem., Int. Ed. Engl.* **1995**, *34*, 798−800.
(28) Rebierre, F.; Riant, O.; Kagan, H. B. *Tetrahedron: Asymmetry* **1990**, *3*, 199−214.

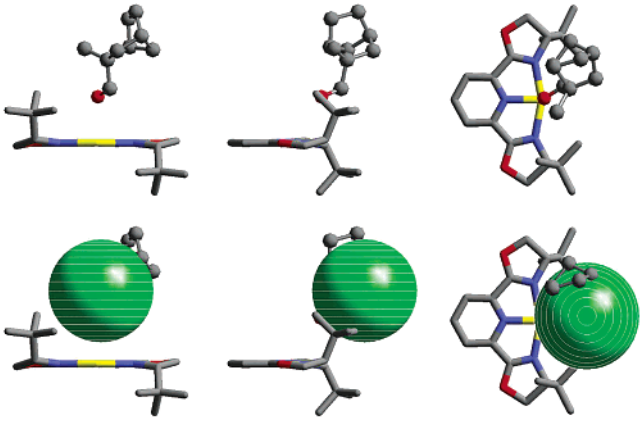

Figure 23. Location of transition-state probe and region of maximum stereoinduction for catalyst **14**. See caption of Figure 9 for details concerning the graphic.

Koga.[29] The researchers chose aluminum alcoholate complexes where an oxygen is in the vicinal position of the alkoxide moiety. Kagan's group hoped that the vicinial oxygen would chelate with the aluminum, providing a bidentate binding chiral ligand. Kagan's group chose the Diels−Alder reaction of methacrolein with cyclopentadiene as a standard reaction by which to judge chiral aluminum complexes. Kagan's group started with a noneffective chiral Lewis acid catalyst (S)-2-methyl-1-phenyl-1,2-dihydroxypropane·$AlCl_2$ (catalyst **16**) and optimized that to an effective one (S)-1,1-diphenyl-1,2-dihydroxypropane·$AlCl_2$ (catalyst **15**). Kagan proposes that the active catalyst is the monoalcoholate structure. NMR data suggests that the catalyst oligomerizes as temperature rises from −78 °C to room temperature. Also, as the reaction temperature rises, the resulting enantioselectivity declines. The researchers correlate the loss of enantioselectivity to the loss of active monoalcoholate catalyst because of oligomerization. If both catalysts conform to the working hypothesis, catalyst **15** (ee = 73%) should have the site of chemistry near the region of maximum stereoinduction while catalyst **16** (ee = 0%) should lack the spatial congruence of these sites.

Catalysts **15** and **16** were generated from a dimer X-ray structure in the CSD. Bis-(μ_2-(S)-(−)-1,1-diphenyl-1-hydroxypropane-2-olato)-dichloro-aluminum is the CSD X-ray dimer that served as the progenitor to the catalyst structures used in our mapping. The monomer structures comprising the dimer are not the same. One monomer has a positive dihedral angle for the O−C−C−O atoms while the other monomer has a negative dihedral angle. For this system, then, there exist stereogenic centers in addition to ligand backbone twisting (P and M) giving rise to diastereomers. We separated the monomer structures from the X-ray dimer structure by breaking the connecting bonds and then geometry optimized each structure to determine the most stable monomer structure. The monomer having the negative dihedral angle had a lower heat of formation and was used by us to create the catalyst models (once the correct methyl and phenyl substituent patterns were introduced). The chirality mapping results are presented in figures S24 and S25 for catalysts **16** and **15**, respectively (see Supporting Information). What is most interesting in these plots is that the ineffective catalyst has a distance between the site of chemistry and the region of maximum stereoinduction ~12 Å while the effective catalyst has these sites separated by ~3 Å. The structural modifications made by Kagan, which are manifest in his experimental results, show up nicely in the mapping methods described here.

(29) Hashimoto, S.; Komeshima, N.; Koga, K. *J. Chem. Soc., Chem. Commun.* **1979**, 437−438.

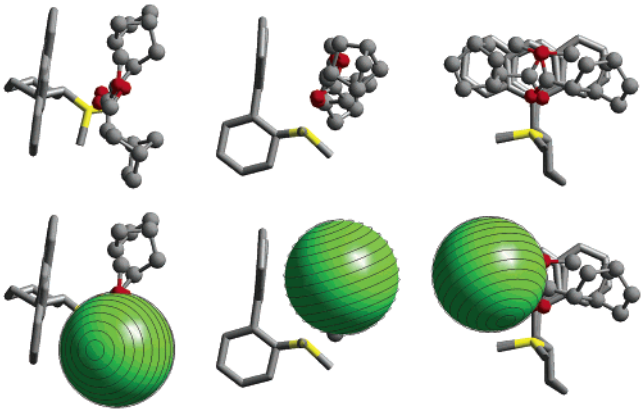

Figure 27. Location of transition-state probe and region of maximum stereoinduction for catalyst **17**. See caption of Figure 9 for details concerning the graphic. In the diagram, two conformational states of the catalyst along with two transition-state probes are depicted. It is difficult to see the two orientations of the naphthyl rings in the left two frames; a better view can be seen in the right-hand frames.

Catalyst 17. We now consider the two cycloaddition reactions from Scheme 3. Hawkins et al.[30] studied a highly effective chiral Lewis acid catalyst, dichloro-(2-(naphthyl)cyclohexyl)borane, catalyst **17**. He found **17** to be a highly effective chiral catalyst for the Diels−Alder reaction of methyl acrylate with cyclopentadiene while run in dichloromethane. There exists X-ray data for a related **17**·dienophile intermediate complex, dichloro-(2-(naphthyl)cyclohexyl)-(methyl crotonate)-borane (CSD refcode KOHFUI). Removal of methyl crotonate followed by conformational analysis gave rise to two conformers within ~1 kcal/mol of each other and differing only in the relative orientation of the naphthyl ring (see below). Both conformers were used in the mapping procedure. One of the transition-state probes used in this analysis is presented in figure S26 (Supporting Information). The same mapping procedures used above were implemented again here and the result of our analysis is presented in Figure 27. In this figure, it is somewhat difficult to discern the two naphthyl ring conformers because they lay in the same plane. Nonetheless, both conformers are present (along with their associated transition-state probes) in the diagram. Again there exists a spatial congruence between the most stereoinducting region of the catalyst and the site of chemistry.

Catalyst 18. Yamamoto et al.[31] sought to develop chiral organoaluminum Lewis acid catalysts for the Diels−Alder reactions of α,β unsaturated esters with cyclopentadiene. α,β unsaturated esters as dienophiles have low reactivity for Diels−Alder cycloaddition reactions relative to α,β unsaturated aldehydes and oxazolidines. Yamamoto found (R)-(+)-3,3′-bis-(triphenylsilyl)-1,1′-bi-2-naphthol-aluminum-methyl, catalyst **18**, to be weakly enantioselective for the Diels−Alder cycloaddition reaction of methyl acrylate with cyclopentadiene. We are interested in this ligand because of its poor performance relative

(30) Hawkins, J. M.; Loren, S. *J. Am. Chem. Soc.* **1991**, *113*, 7794−7795.
(31) Maruoka, K.; Concepcion, A. B.; Yamamoto, H. *Bull. Chem. Soc. Jpn.* **1992**, *65*, 3501−3503.

to **17**. Catalyst **18** was generated from an X-ray structure in the CSD with a similar chiral ligand. (m_2-1,1′-Bi(2-naphtholato))-(1,1′-bi(2-naphtholato))-cyclohexanone-O-bis(tetrahydrofuran)·aluminum·lithium·tetrahydrofuran (CSD refcode ZOHVIB) is the structure that served as the progenitor to **18**. We removed everything except one 2-naphtholato chiral ligand and the chelated aluminum. We added triphenylsilyl substituents to the twisted biaryl ring and a methyl group to the aluminum. Having made extensive structural modifications, we then geometry optimized **18** using the PM3(tm) Hamiltonian. The results of our mapping are presented in figure S28 (Supporting Information). In this example, the most stereoinducing region around the catalyst is 8.96 Å from the site of chemistry.

Discussion

A need exists for generating efficient chiral catalysts, yet there are few design strategies available for this purpose. One approach is the brute-force attempt to make as many molecules as possible for testing via combinatorial design strategies, but even this requires some kind of assessment of what ligand modification to try and what not to try. The most common approach in the catalyst design community appears to be one of trial and error. Here, one first finds a reasonable "lead" catalyst. Then, using intuition or chemical knowledge derived from mechanistic studies of the reaction being catalyzed, one attempts to optimize the lead catalyst by placing suitable substituents on the substructure of the initial lead catalyst (and modulating effectiveness by changing solvent, metal, lability of associated counterions, temperature, etc.). Rarely is ligand design done de novo. Regardless how one designs new catalysts, the point raised in this paper is that catalysts lacking an immediate chiral environment around the site of chemical reaction (top diagram of Figure 2) will result in little or no enantioinduction. A suitable chiral microenvironment is needed at the site of chemistry.

Having this chiral microenvironment at the site of chemical reaction does not, in itself, mean good enantioinduction will be achieved experimentally, however, because other interfering, debilitating factors may be operative. Nonetheless, the chirality of the catalyst needs to be where the chemical reaction is taking place. In this research project, we examine this issue by presenting a hypothesis stating that the stereoinducing efficacy of a catalyst is maximized when there exists a spatial congruence between the site of chemical reaction and the catalyst's region of maximum stereoinduction. The trend we would expect to see, in general, is that catalysts that are efficient at asymmetric induction will have these regions spatially congruent but ineffective catalysts will not. This may seem an obvious assertion but until now there has been no mention of it in the literature nor has there been a way to assess it.

The catalysts selected for proving or disproving this hypothesis were chosen because they are well-studied reactions that have been "optimized" , that is, accountability exists for solvents, counterions, and the like by the research groups who developed those catalysts. The reported ee's for these catalysts are thus considered by us to be reliable enough for computational study. We are cognizant that the reported ee's still may not be the best numerical values possible so we simply categorize the catalysts here as being either efficient or inefficient and then see if our working hypothesis holds for this categorization. The three sets of reactions presented in Schemes 1−3 are all Diels−Alder reactions. We selected this particular group of Diels−Alder reactions because they have relatively well-defined transition states that are amenable to calculation and because they represent important chemical reactions in synthetic organic chemistry. In this paper, a set of 18 different catalysts were assessed and all but one example conforms to the working hypothesis.

The first set of catalysts studied (Figure 5) include a diverse set of ligands, organic functionality, and metals, and they contain five-, six-, or seven-member metal-containing rings. This is a truly diverse and representative set of catalysts to evaluate. Catalysts **1**−**7** are all efficient at carrying out the Diels−Alder reaction of cyclopentadiene with 3-acryloyl-1,3-oxazolidin-2-one, meaning they effectively induce high levels of stereoselectivity. Contrarily, catalysts **8**−**11** do not. If the posited hypothesis has any merit, one should find a spatial congruence between the region of maximum stereoinduction for the former set of catalysts but not for the latter set. This finding is observed with the exception of catalyst **5**. In the original paper describing the synthesis, testing, and mechanistic interpretation of that catalyst, Evans indicated that the stereochemical outcome is consistent with a four-coordinate, square-planar Cu(II) geometry and accompanying *s-cis* dienophile geometry (as depicted in Figure 13). Evans acknowledged a less-likely possibility where the observed sense of stereoinduction arises from a tetrahedral metal center and an *s-trans* dienophile conformation. We tried Evans' less-likely possibility in our mapping (results not shown) but that too gave inconsistent results. We cannot rationalize why this example does not conform to the hypothesis.

The catalysts **8**−**11** all have the region of maximum stereoinduction distant from the site of chemical transformation, a result that conforms to the hypothesis. Of special interest are the catalyst systems **1** and **8** as well as **6** and **11**. Changing the phenyl group on **1** to a methyl group renders it ineffective (catalyst **8**); this is an experimental fact that is paralleled here computationally. Likewise, changing the large substituents on **6** to smaller substituents renders it inefficient (catalyst **11**) and this too is accounted for by our hypothesis. The catalyst pair **5** and **10** cannot be commented on here because we get an inconsistent result for catalyst **5** but a consistent result for **10**.

The second reaction system we studied is the Diels−Alder reaction of cyclopentadiene with acrolein and methacrolein (Scheme 2). Again, a diverse set of metals, ligands, and types of metallocycles are assessed and in all cases our mapping results conform to the hypothesis. Most interesting is the set of catalysts **15** and **16** with the former being an effective catalyst but the latter being ineffective. Again the computational results parallel this finding.

The last system evaluated is the catalyzed reaction of cyclopentadiene with methylacrylate (Scheme 3). Catalyst **17** is efficient at asymmetric induction while catalyst **18** is not. The stereocartographic results are consistent with the hypothesis for this reaction too. Hence, given a related series of Diels−Alder reactions carried out by a diverse set of 18 chiral coordination complexes used as Lewis acid catalysts, we find that 17 of them conform to the hypothesis.

Because we are able to evaluate where the most stereoinducing region for a given catalyst exists relative to where the chemistry is actually taking place, we attempted to correlate

the observed ee with the distance between those two regions. We were not able to find a statistically meaningful correlation. This was not unexpected because the reported ee's may not be right (some of the lower ee's, under more favorable conditions, might give higher values) but also because of how we did the mapping study. In particular, we did not always carry out geometry optimizations for catalysts derived from the CSD nor did we account for soft ligand distortion modes in a dynamically averaged way, which may be important (though we do account for different conformational states). Moreover, we assumed that counterions are not intimately involved in the reaction process by moving them infinitely far from the catalyst in our models. But, while a linear relation between ee versus distance separating these sites could not be found with these assumptions, we can say that 17 of the 18 examples do conform to the hypothesis. What this means is that one can now predict, in a "yes"/"no" way, whether a given catalyst will be effective at asymmetric induction for a particular reaction with a 94% probability of being right.

Summary

Holz et al.[32] have lamented "...in spite of literally thousands of chiral ligands that have been reported in the past, there is no unique rationale for the efficiency of all catalysts not even for those that have been applied in the same reaction. Therefore the design of new catalysts is based on trial and error." This comment reflects the state-of-the-art in ligand design. One overriding view of catalytic stereoinduction is that highly effective chiral catalysts should maintain a spatial congruence between the site of "chemistry" and the region of greatest stereoinduction and a hypothesis to this effect was posited for testing. At the very least, efficient catalysts must have this congruence. Inefficient catalysts may have those sites being congruent but other interfering factors may ruin the potential for stereoinduction (or those inefficient catalysts may simply lack the requisite spatial congruence that would otherwise make them efficient). In this paper, we developed a computational method for assessing the region of maximum stereoinduction. Because this is a simple mapping process, we call the concept "stereocartography". The key point about this mapping procedure is that it is based on energy calculations using well-known potential energy functions. Moreover, rather than using an arbitrary, generic, or "universal" probe, the probes used to map these stereodiscriminating regions are the actual transition states of each catalyzed reaction under study.

Seventeen of eighteen catalysts studied conform to the hypothesis. This, in its own right, suggests the method can determine whether a proposed catalyst will be efficient or whether it will be inefficient at carrying out its stereodiscriminating task. The methodology is simple and broadly applicable. Therefore, it has much promise as a strategy for the design of chiral catalysts. Moreover, because the method uses grid-based sampling, one can easily implement it on a Beowulf cluster as we have or even on a loosely knit cluster of machines, worldwide, in the spirit of what Richards and others have done recently.[33] The posited hypothesis has been tested and, with one exception, affirmed. While these results are promising, we point out that only a single class of reactions has been used to test the hypothesis. Further work on this concept is thus justified and in progress.

Acknowledgment. This work was funded by grants from the National Science Foundation (CHE 992888) and the Petroleum Research Fund, administered by the American Chemical Society (35172-AC4).

Supporting Information Available: Figures S11, S14, S15, S17−S22, S26, S28, as described in the text (PDF). This material is available free of charge via the Internet at http://pubs.acs.org.

JA0207192

(32) Holz, J.; Stürmer, R.; Schmidt, H.-J.; Heller, D.; Krimmer, H.-P.; Börner, A. *Eur. J. Org. Chem.* **2001**, 4615−4624.

(33) (a) Cha, A. E. *Washington Post*, Feb 21, **2002**, p E06. (b) See the website on In-Silico Screening for Anthrax Toxin Inhibitors: http://www.chem.ox.ac.uk/anthrax/. (c) For more about high throughput computing using collections of distributively owned computing resources see, e.g., Condor website: http://www.cs.wisc.edu/condor.